Heliyon 9 (2023) e20676

Contents lists available at ScienceDirect

Heliyon

journal homepage: www.cell.com/heliyon

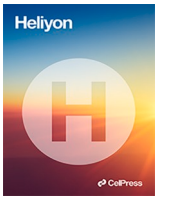

Zinc oxide nanorod/rutin modified electrode for the detection of Thiourea in real samples

M.A. Khaleque [a,b], M.R. Ali [a,b], M.S. Bacchu [a,b], M.R.A. Mamun [a,b], M.I. Hossain [a,b], M.S. Hossain [a,b], Mohamed Aly Saad Aly [c,**], M.Z.H. Khan [a,b,*]

[a] *Dept. of Chemical Engineering, Jashore University of Science and Technology, Jashore, 7408, Bangladesh*
[b] *Laboratory of Nano-bio and Advanced Materials Engineering (NAME), Jashore University of Science and Technology, Jashore, 7408, Bangladesh*
[c] *Department of Electrical and Computer Engineering at Georgia Tech Shenzhen Institute (GTSI), Tianjin University, Shenzhen, Guangdong, 518055, China*

ARTICLE INFO

Keywords:
Thiourea
Zinc oxide nanorod
Electrochemical detection
Rutin modified sensor
Real samples analysis

ABSTRACT

In this work, a novel electrochemical detection strategy was developed based on a metal-organic framework of zinc oxide nanorod nanoparticles and rutin for selective screening of Thiourea as toxic chemicals. The zinc oxide nanorod were synthesized by following direct chemical precipitation methods and characterized by X-ray diffraction and X-ray photoelectron spectroscopy analysis. The surface of modified electrodes was also characterized by field emission scanning electron microscopes, energy-dispersive X-ray spectroscopy, and attenuated total reflectance flourier transform infrared spectroscopy. Furthermore, the electrochemical activity of the developed sensor was tested by cyclic voltammetry, differential pulse voltammetry, and electrochemical impedance spectroscopy. The modified electrode showed outstanding electrocatalytic activity towards the detection of Thiourea in phosphate buffer saline at a high pH level of 12.0. The proposed sensor showed a linear range of linearity in a concentration ranging from 5.0×10^{-6} - 900×10^{-6} molL^{-1} and a detection limit of 2.0×10^{-6} molL^{-1}. Moreover, the selectivity of the developed electrochemical sensor was investigated for the detection of Thiourea in the presence of organic compounds and a group of anions. Furthermore, the proposed strategy demonstrated an excellent recovery value in the spiked farmland water and fruit juice sample.

1. Introduction

Thiourea (TU) is used as fungicide, herbicide and rodenticides in agricultural applications [1]. Mostly, it can cause cancer [2], cause allergic reactions [3], give rise to a disturbance effect on carbohydrate metabolism [4], induce hypothyroidism [5] and has an antibacterial effect against nitrifying bacteria [6,7]. According to world health organization (WHO) the acute toxicity lethal dosages (LD_{50}) of TU is 125–1930 mgkg^{-1} body weight (bw) for rates (oral), the dermal LD50 is $>$ 2800 mgkg^{-1} bw, and the inhalation lethal concentration (LC_{50}) is $>$ 195 mgm^{-3} in rates, up-taking 10 % solution in 4 h [8]. Besides, TU is used in the synthesis of metals such as copper, paint industries, the production of textiles, pharmaceuticals, rubber, and papermaking [9]. Furthermore, TU is used to protect the early ripening of various fruits [10] and treating grain [11], as a seed priming agent, for normal plant growth, and as fertilizer [12,

* Corresponding author. Dept. of Chemical Engineering, Jashore University of Science and Technology, Jashore, 7408, Bangladesh.
** Corresponding author.
E-mail addresses: mohamed.alysaadaly@ece.gatech.edu (M. Aly Saad Aly), zaved.khan@yahoo.com (M.Z.H. Khan).

https://doi.org/10.1016/j.heliyon.2023.e20676
Received 8 May 2023; Received in revised form 23 September 2023; Accepted 4 October 2023
Available online 4 October 2023
2405-8440/© 2023 Published by Elsevier Ltd. This is an open access article under the CC BY-NC-ND license (http://creativecommons.org/licenses/by-nc-nd/4.0/).

13]. Thus, TU might be present in industrial effluent water, agricultural field water, sewage water, processed foods, juices [10,14] and they also contaminate underground water [15]. In spite of some significant benefits in the above fields, TU is known as a typical contaminant in all applied fields of agrochemicals [16]. Therefore, TU and its derivatives are considered chemical hazardous and toxic substances and should be banned in all applications (see Schemes 1–3).

Numerous analytical techniques were reported for the detection of TU for food, portable water, and environmental pollutant analysis. Flow injections method [17], Raman spectrometry [18], spectrophotometry [19], mass spectrometry [20], polarography [21], stripping voltammetry [22], high performance liquid chromatography [23], FTIR spectrometry [24] and electrochemical methods [25–29] are the existing methods for the detection of TU. Most of these techniques are time-consuming, expensive, nonselective, expensive, and insensitive. In contrast, the electrochemical techniques are more advantageous for detecting different trace levels of TU due to their high linearity, superior selectivity, outstanding sensitivity, and they are easy to handle [30–32]. *Iraj Jodan and* et al., reported a research work for TU detection on silver and poly (alizarin) polymer modified surface. In this study, they found the limit of detection (LOD) 3.3×10^{-6} molL^{-1}, and a linearity 1.0×10^{-5}-9.40×10^{-4} molL^{-1} [33]. Another research work was done to detect TU as hazardous toxin with sandwich type CuO/ZnO Nanospikes/Nafion composite modified GCE. As a research outcome, they are able to detect a linear range between 1.5×10^{-4} to 1.20×10^{-3} molL^{-1} TU with $23.03 \pm 1.15 \times 10^{-6}$ molL^{-1} of LOD [34]. Additionally, chitosan was decorated with photo chemically reduced silver nanoparticles for Ag@CTSN nanocomposite preparation and electrode modification for the detection of TU. Here, the detection linearity was shown (2.0×10^{-4}-3.6×10^{-2} molL^{-1} and LOD of 1.8×10^{-5} molL^{-1} [35]. In spite of different reported research outcome, we have already developed totally new sensor for electrochemical detection of TU in this study for real analysis.

Metal oxide nanomaterials exhibited unique properties differing from bulk materials, initiating from their quantum-scale measurements. Numerous applications in analytical techniques utilized metal oxide nanoparticles to construct electrochemical sensors and biosensors [36,37]. It is noteworthy that metallic nanoparticles have excellent photonic and electronic properties [38]. Zinc oxide nanorods (ZnONRs) exhibit moderate electrical and thermal conductivity and they are highly reactive [38,39]. These properties are dependable on simplicity of the fabrication, well-regulated shape and size, nontoxicity, the presence of extrinsic and intrinsic at the emission center [40,41]. The modified ZnONRs behave as efficient electrochemical sensor due to their biocompatibility, high-level of surface energy and large surface area, superior catalytic efficiency, great adsorption ability, high isoelectric point, and natural abundance [38,42–45]. Moreover, ZnO nanoparticles have also extensive applications for the development of electrochemical sensor [46–48]. The sensitive detection of paracetamol was also done using ZnO modified GCE [38,49]. Another research, 5 % barium-doped ZnO nanoparticles was used to modify GCE for the electro-oxidation of nimesulide [50]. ZnO nanoparticles was also used for the electrochemical detection of triclosan [51], ascorbic acid [52–54], methyl-parathion [39], uric acid [54,55], glucose [56], dopamine [57] and others. In this study, we select hydrothermally synthesized ZnONRs as an electro catalyst and increase the oxidation rate of TU.

Rutin is a polyphenol compound found in many medicinal plant and vegetables. This –OH modified compound has a strong propensity to be adsorbed onto the ZnONRs surface by dipole attraction [58,59]. Such adsorption is created by developing a chemical interface with structurally well-defined and stable monolayers called self-assembled monolayer (SAMs) [60]. These SAMs act as intermediate layers during the accumulation and later the reaction with the target analyte. Furthermore, they can improve the properties of the modified electrode surface in terms of sensitivity and selectivity [61]. In previous reported research work rutin have modification of electrode for preparation of electrode for electrochemical oxidation of variety of analyte [62–64]. Moreover, modifying the surface using ZnONRs can mainly boost the immobilized amount of rutin and enhance the stability of SAM layers [65–69]. The selection of rutin as a mediator which enhance the oxidation of TU.

In the present study, we have synthesized, characterized, and applied the hydrothermally synthesized the ZnONRs to modify the

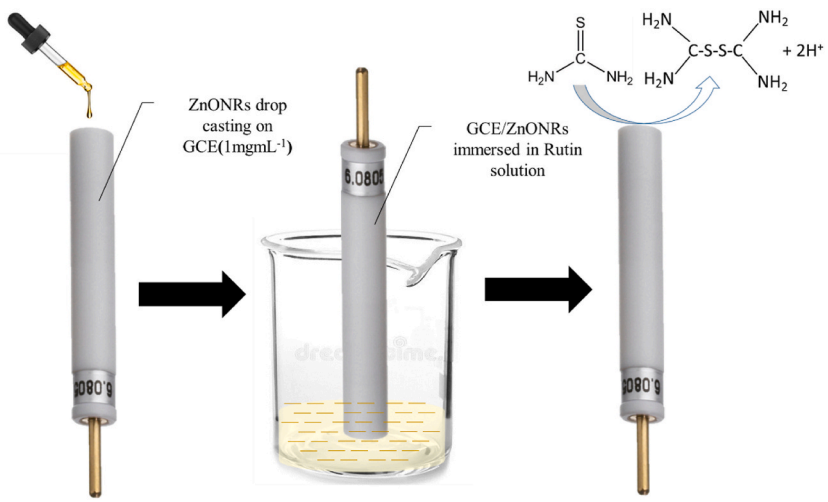

Scheme 1. Systematic representation for the preparation of GCE/ZnONRs/Rutin and detection of TU.

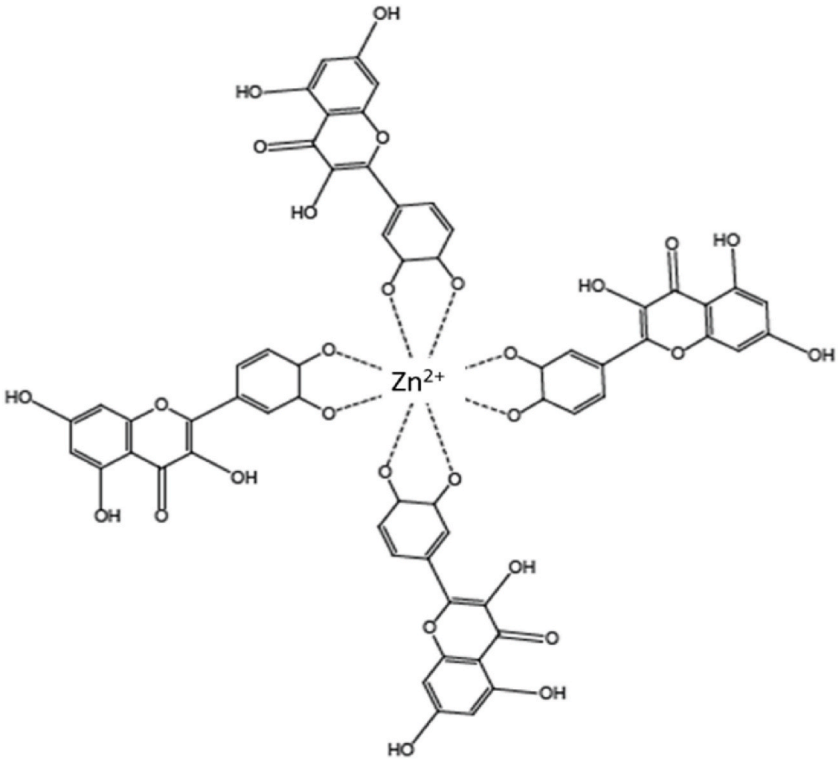

Scheme 2. Possible covalent bond formation between rutin and zinc ions (ZnONRs) at 65 °C.

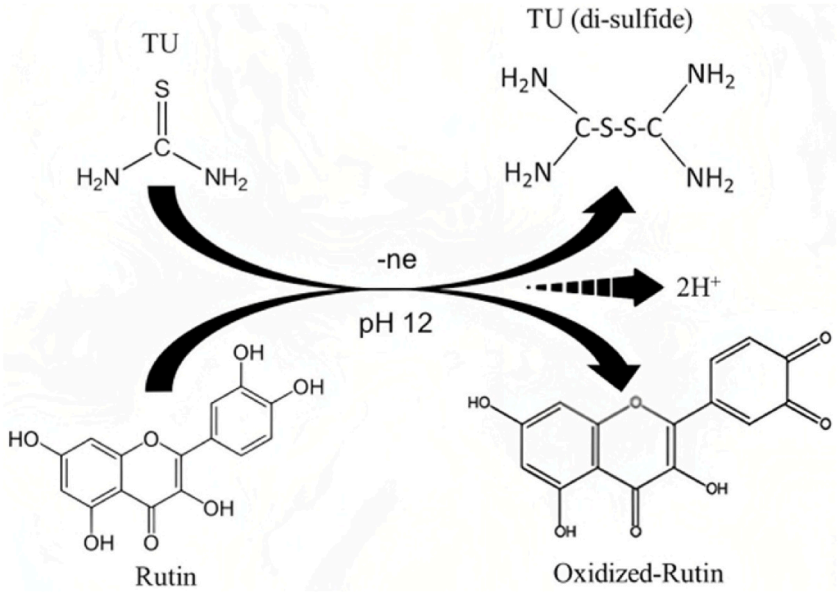

Scheme 3. The proposed oxidation mechanism of TU at the surface of GCE/ZnONRs/Rutin.

GCE/ZnONRs/Rutin. For the detection of TU, ZnONRs is functionalized with rutin which act as an electrocatalyst on ZnONRs. Due to the moderate covalent bonding attraction of ZnONRs and rutin the ZnONRs/Rutin composite electrode is chosen for oxidation of TU. The developed sensor totally new the existing reported sensor which is simple, and easy to modify. The modified sensor have an excellent limit of detection of 2.0×10^{-6} molL^{-1} with having a long range of linearity 5.0×10^{-6}-9.0×10^{-4} molL^{-1} than previous research work ever. In this experiment, we found an optimum pH 12.0 of maximize oxidation of TU. Furthermore, farmland water, and drain water, analysis medium was also exhibited excellent result which is better than previous reported research wok. The selectivity

result in inorganic medium was also good.

2. Materials and methods

2.1. Chemicals and materials

All of the chemical substances were all of analytical grade. Zinc nitrate $Zn(NO_3)_2{\cdot}6H_2O$ was obtained from Loba Chemie Pvt. Ltd. (India), Sodium hydroxide (NaOH) from Merck, Germany, rutin ($C_{27}H_{30}O_{16}.3H_2O$) from Aladdin Chemistry Co. Ltd. (China), and Thiourea (CH_4N_2S) Merck life science Pvt. Ltd. (India). A supporting electrolyte of phosphate buffer saline (PBS) was purchased from Sigma Aldrich (China). Type-I ultrapure water (resistivity <18 MΩ) was made from Evoqua water technologies (Germany). All analytical solution and electrolyte bath were prepared by using this deoxygenated ultrapure water.

2.2. Synthesis of ZnONRs

ZnO nanoroads were synthesized by direct precipitation method. At first 200 ml of $Zn(NO_3)_2{\cdot}6H_2O$ (6.0×10^{-3} molL^{-1}) was prepared with continues stirring. Successively, the alkali NaOH solution (0.4molL^{-1}) was slowly added into the mixture under vigorous stirring and at room temperature until a white suspension was formed. Next, the white suspension was precipitated after centrifugation for 10 min at 6000 rpm. Following, the precipitation was washed several times with ultrapure water and one time with 100 % ethanol. The obtained suspension was dried at 140 °C in a dryer for 6 h and then was labelled as ZnONRs.

2.3. Fabrication of the GCE/ZnONRs/Rutin

Before electrode modification, the bare GCE was polished over a velvet micro-cloth with 1.0 μm, 0.3 μm and 0.05 μm alumina slurry. Next, the electrode was ultra-sonicated in ultrapure water, ethanol, and 1:1 nitric acid bath for 2 min. Finally, the electrode surface was dried by nitrogen gas flow. To prepare GCE/ZnONRs, 1 mg of ZnONRs was dissolved in 1.5 ml ethanol under ultra-sonication for 30 min. Then, 10 μl of suspended nanoparticles was coated on the surface of neutralized GCE surface and then left to dry at 60 °C for 5 min.

To make the GCE/ZnONRs/Rutin, 10 ml of 1×10^{-3} molL^{-1} rutin solution was prepared by mixing rutin with ultrapure water under agitation with magnetic stirrer forming a homogeneous mixture. The dried GCE/ZnONRs electrode was immersed in the homogeneous mixture for 20 min under a temperature level of 65 °C. Thereafter, the electrode was withdrawn and rinsed with double distilled ultrapure water with care and then it was ready to use. The modified electrode was denoted as GCE/ZnONRs/Rutin electrode. The total working procedure for the modification of GCE is represented in Fig. S1.

2.4. Apparatus and instruments

In this experiment, all glassware was treated with 10 % nitric acid for 24 h and dried at 60 °C. Electrochemical measurement was

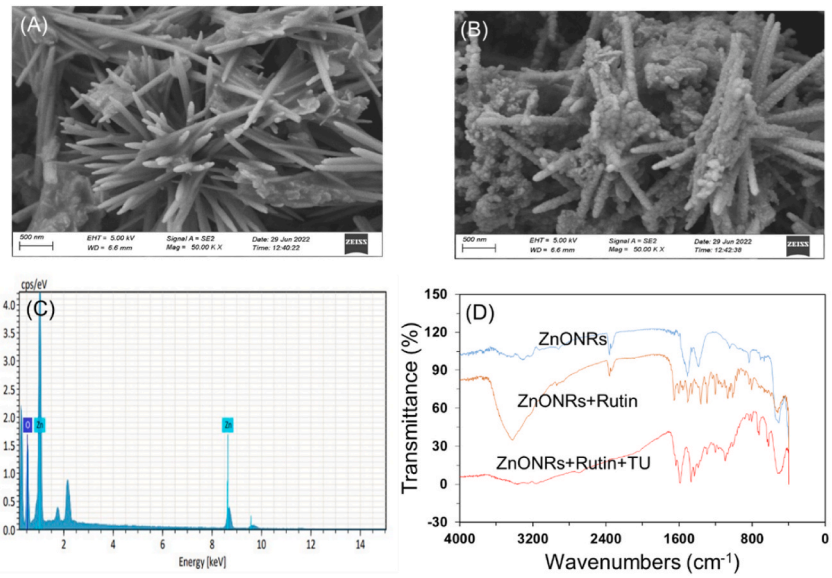

Fig. 1. SEM images of (A) bare GCE/ZnONRs; (B) bare GCE/ZnONRs/Rutin; (C) EDX analysis of ZnONRs where the bright spot show the distribution of Zn and O elements on the electrode (D) ATR-FTIR spectrum of ZnONRs, ZnONRs + Rutin, ZnONRs + Rutin + TU.

performed using an electrochemical workstation (Corrtest CS300, China). The EcoSense®pH1000A bench top was used as pH meter. The surface topography with individual elements was characterized by scanning electron microscopy (ZEISS Gemini SEM 500, UK) and attenuated total reflectance flourier transform infrared (ATR-FTIR, NICOLET iS20) spectroscopy. The electrochemical impedance spectroscopy (EIS) measurements was conducted on Metrohm DropSens (μStat-I 400 s S/N: IS4091044A) machine.

The crystal structure studies were analyzed using X-ray diffraction (XRD) patterns (RINT2200, Rigaku, Japan) in the 2θ range of 20–80° with a scan rate of 0.02°/S at the surrounding temperature. The diffract grams were recorded with a Cu-Kα radiation tube at control configurations of wavelength of λ: 0.15406 nm, voltage of 45 kV, and current of100 mA. The average crystalline size of all samples were calculated using Debye-Scherrer formula. The lattice parameters were also calculated using a tetragonal formula based on miller indices.

The study of binding energy and the new chemical state of all sample's surfaces was performed by X-ray photoelectron spectroscopy (XPS) (PerkinElmer, PHI 5600 XPS MA, USA), at a base pressure in the analysis chamber of 4.0×10^{-8} Pa (during measurement pressure 1×10^{-7} Pa), Al Kα X-ray source excitation energy $h\nu = 1486.6$ eV & 200 W has been used. The sample was positioned at an angle of $\theta = 45°$ between the input lens of the analyzers and the surface normal. The analyzer's energy calibration has been performed with Au $4f_{7/2}$ core peaks at 84.0 eV with a resolution of 0.125eV.

3. Results and discussions

3.1. Surface morphology and functional group study

The surface morphology with elemental composition and functional groups of the prepared electrode surface is shown in Fig. 1. A rod-like surface morphology was demonstrated as can be seen in Fig. 1A. A relatively rough surface and irregular shape with uniform distribution were exhibited with the addition of rutin in ultrapure water as shown in Fig. 1B. The average diameter was measured and found to be 50–100 nm for ZnONRs.

The peak observed at 507 cm^{-1} corresponds to the stretching vibration of ZnONRs, as shown in Fig. 1C [70,71]. The observed peaks at 668.70 and 835.31 cm^{-1} denote the stretching vibration of ZnONRs Zn–OH [71,72]. The Peaks at 1386.40, 1457.96, and 1507.45 cm^{-1} indicate the nitro groups. The peaks at 1047.13 and1653.87 cm^{-1} represent the symmetric and anti-symmetric modes of C–O [73,74]. The rest of the peaks at 3442.04, 3310.53, 2360.59, and 2342.75 cm^{-1} can be designated to the stretching vibrations of the OH groups [75]. In addition, ZnONRs and rutin composite has shown multiple vibrations with a broad spectrum from 409.60 to 3903.50 cm^{-1}. It is noteworthy that there was no noticeable chemical complex between ZnONRs and rutin, however, a dipole interaction of –OH and Zn^{2+} and a peak at 668.65 cm^{-1} of Zn–OH were observed. Similarly, after the addition of TU in the mixture of ZnONRs and Rutin, there was no significant changes observed except a Zn–OH stretching vibration remained at 668.65 cm^{-1} [71,72].

Based on the energy-dispersive X-ray spectroscopy (EDX) analysis of the ZnONRs, it was proven that the electrode surface was decorated with nanorods. The EDX surface distributions confirmed the presence of Zn and O as shown in Fig. 1D.

As shown in Fig. 2 elemental mapping of the modified electrode surface are represented from A to G. where separate color represent

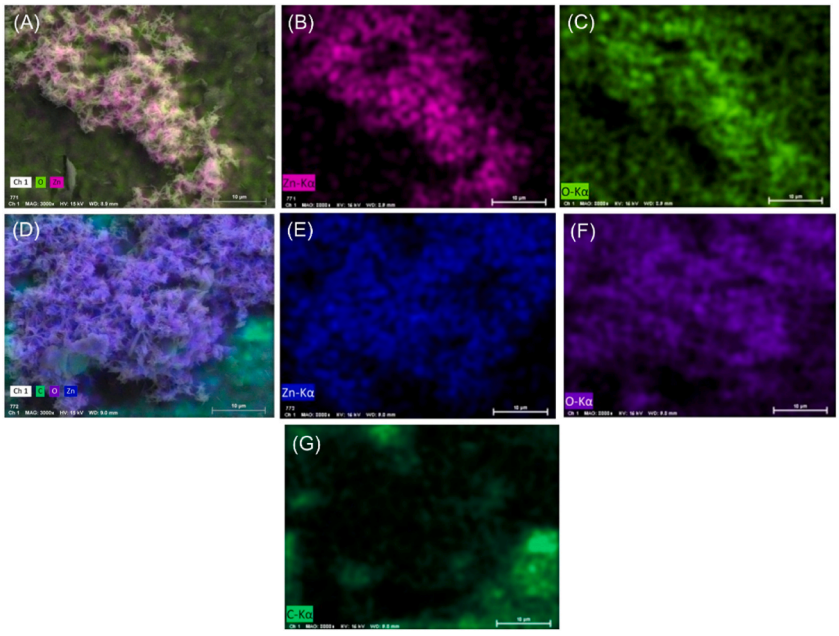

Fig. 2. EDX elemental mapping of (A): Zn, O; (B): Zn; and (C) O of GCE/ZnONRs modified electrode surface. (D): Zn, O, C; (E): Zn; (F): O; (G): C of GCE/ZnONRs/Rutin modified electrode.

individual elements mentioned in title.

Fig. 3A depicts the XRD patterns of all samples to determine the crystal phase, crystallinity, and phase purity. As shown in Fig. 3A, the 2θ peaks of 31.70°, 34.38°, 36.16°, 47.46°, 56.52°, 62.81°, 66.35°, 67.91°, 69.11°, 72.64°, and 76.96° correspond to the {100}, {002}, {101}, {102}, {110}, {103}, {200}, {112}, {201}, {004}, and {202} (JCPDS file card 36–1451) diffraction planes of hexagonal wurtzite phase of ZnO [76].

The Debye Scherrer formula stated in Eq. (1) where λ is the wavelength of the X-ray radiation, θ is the diffraction angle of Bragg, β is the width at half maximum (FWHM) peak, and K (0.89) is the Scherer constant, respectively. The crystalline size (average) was calculated and found to be 17.21 nm for ZnONRs.

$$D = \frac{K\lambda}{\beta \cos\theta} \tag{1}$$

the crystal lattice parameters were computed using Eq. (2), where d is the lattice spacing of inter-planar distance, h, k, and l are the miller indices, and a and c are the lattice parameters. The estimated lattice parameter values were found to be a = 3.2534 Å and c = 5.6351 Å for the pure ZnO NRs.

$$\frac{1}{d^2} = \frac{4\left(h^2 + hk + k^2\right)}{3a^2} + \frac{l^2}{c^2} \tag{2}$$

A XPS wide spectra survey of ZnONRs is shown in Fig. 3B, in which Zn, O and C were detected in the three wide survey spectra. The detected carbon is not from the added chemicals, it is from the ambient atmosphere. All binding energies were corrected from the charge shift using the C 1s peak of graphitic carbon (BE = 284.6 eV) as a reference [77].

Here, in the core level XPS spectra of ZnONRs nanostructures are shown in Figure Fig. 3C. As shown in the figure, the observed peaks for Zn $2p_{3/2}$ and $2p_{1/2}$ at binding energy of 1021.2 and 1044.2 eV respectively, with peak separation of 23.0 eV, which is similar to previous reports for ZnO nano rods [78–80]. Additionally, The binding energies of 1020.6 eV and 1021.6 eV were attributed to the metal Zn and ZnO, respectively, as shown in Fig. 3D [78]. Similarly, for O 1s, the binding energies of 530.2 eV, 531.1 eV and 532.3 eV are corresponding to ZnO, $Zn(OH)_2$, and CO, respectively (Fig. 3E) [79].

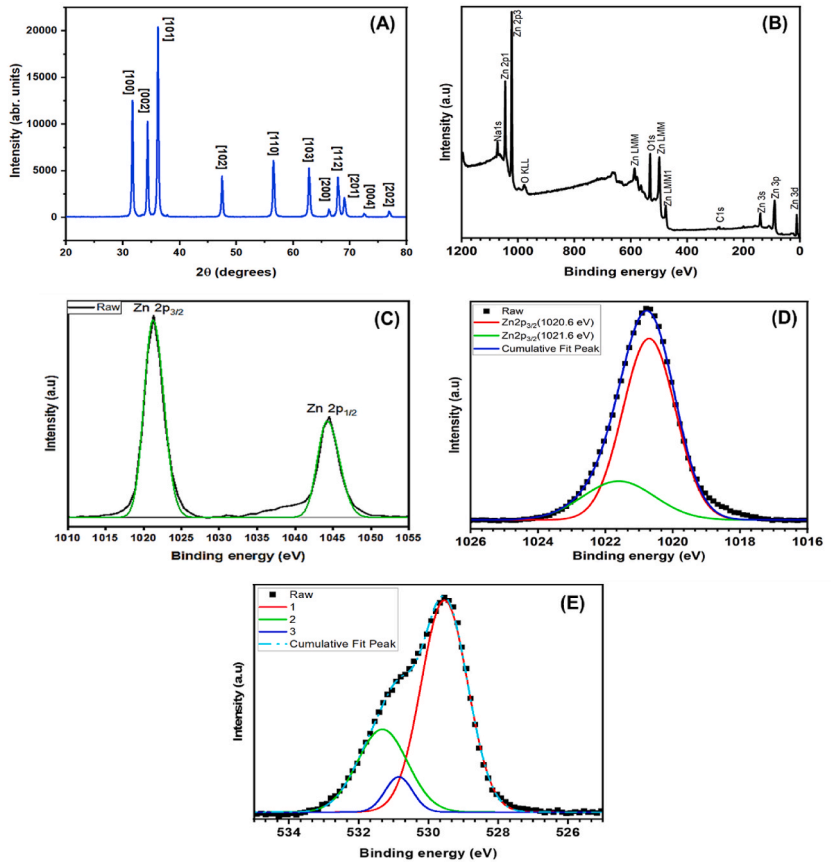

Fig. 3. (A): XRD patterns of ZnONRs; (B): XPS wide survey spectra of ZnONRs; and XPS spectra of (C): Zn $2p_{1/2}$; (D): Zn $2p_{3/2}$ and (E): O 1s.

3.2. GCE/ZnONRs/rutin modification

Ethanol is the most applicable solvent to homogeneous dispersed ZnONRs and for the surface modification. As literature revealed, ethanol can be easily physisorbed on the surface of ZnONRs by forming ethoxy on Zn^{2+} ion or on oxygen vacancies. The physisorbed layer can be formed in a single layer due to the uniform distribution of NRs. During the heating for drying, it was observed that ethanol was molecularly desorbed from physisorbed layers at 145 K. As previously reported, at 250–275 K, chemisorbed ethanol was desorbed and high desorption energy was observed [81–83].

Rutin is a polyphenol compounds contain –OH functional group which have a strong propensity to adsorb onto the surface of ZnONRs by dipole attraction [59,68]. To form well organized ZnONRs-rutin complex, the temperature was maintained at 65 °C for 20 min [60]. The unreacted rutin was easily remove by rinsing with ultrapure water. Then, the modified electrode was ready to use. The possible reaction mechanism are represented in the following Fig. S2.

3.3. Electrochemical behavior of the GCE/ZnONRs/Rutin

As shown in Fig. 4A–D, the electrochemical characterization of bare GCE, GCE/ZnONRs, and GCE/ZnONRs/Rutin electrodes followed by CV in 0.1 $molL^{-1}$ of KCl and 0.005 $molL^{-1}$ of $Fe(CN)_6^{3-/4-}$. By casting an eye on Fig. 4A, the lowest peak current with a well-defined redox peak was obtained for bare GCE with having peak to peak potential separation value (ΔEp) of 162 mV. Furthermore, it was 108 mV for GCE/ZnONRs electrode, and 100 mV for ZnONRs/Rutin modified GCE/ZnONRs/Rutin increasing the diffusion redox rate of $Fe(CN)_6^{3-/4-}$.

As it can be seen in Fig. 4B, the GCE/ZnONRs/Rutin electrode demonstrated the lowest electron transfer resistivity in 0.1$molL^{-1}$ of KCl including 0.005 molL-1 of $Fe(CN)_6^{3-/4-}$ compared with GCE/ZnONRs and bare GCE because of an increase of the active surface area and conductivity of the modified electrode. The semicircle exhibited the highest resistivity, however, the linear line without semicircle showed the lowest resistivity [84,85].

Additionally, the cyclic voltammetry from 0.2 to 0.6 V in 0.1 $molL^{-1}$ KCl including 5.0×10^{-6} $molL^{-1}$ $Fe(CN)_6^{3-/4-}$ solution was done with decreasing scan rate from outer to inner (150, 100, 90, 80, 70, 60, 50, 40, 30, 20, and 10 mVs^{-1}) which is represented in Fig. 4C. It was noticeable that the peak current gradually decreased with minimizing the scan rate. This confirms the ion transfer phenomenon that was controlled by absorption. The corresponding calibration line is shown in Fig. 4D maintaining the rising of oxidation increase and the gradual decrease of reduction current value. These two lines maintained a satisfactory R^2 value. In addition,

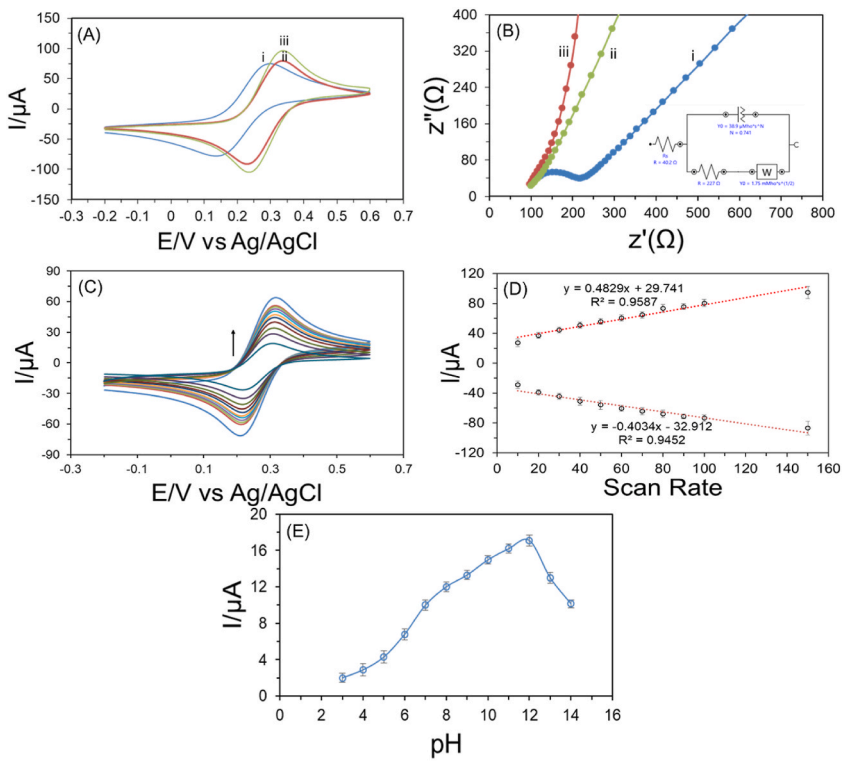

Fig. 4. Cyclic voltammograms of diverse electrodes measurements in 0.1 $molL^{-1}$ of KCl containing 0.005 $molL^{-1}$ of $Fe(CN)_6^{3-/4-}$ (A): (i) bare GCE, (ii) GCE/ZnONRs, and (iii) GCE/ZnONRs/Rutin; (B): EIS images of (i) bare GCE, (ii) bare GCE/ZnONRs, and (iii) GCE/ZnONRs/Rutin (inset: equivalent Randle circuit); (C): CV at diverse scan rates (from outer to inner): 150, 100, 90, 80, 70, 60, 50, 40, 30, 20, and 10 mVs^{-1}, (D) the equivalent calibration plots between distinct scan rates versus cathodic (Ipc) and anodic peak currents (Ipa), (E): pH effect on 5.0×10^{-4} $molL^{-1}$ TU detection.

the developed GCE/ZnONRs/Rutin sensor efficiency in TU solution is also investigated in 1.0×10^{-6} molL^{-1} of CIP solution in PBS (pH 12.0) with varying the scan rate 20, 30, 40, 50, 60, 70, 80, 90, 100, 125, 150, 175, and 200 mVs^{-1}. The obtained data of this analysis is added in Supplementary Information Fig. S1.

Furthermore, pH optimization is reported in Fig. 4E, it plays a crucial factor to get the highest oxidation potential. The DPV was measured in 0.01 molL^{-1} PBS solution of pH level of 2–14. Fig. 4E shows the current of 500×10^{-6} molL^{-1} solution at different pH levels and the DPV response is shown in Supplementary Information Fig. S2. The results of different pH levels of buffer solution increases; the largest current peak that is related to oxidation of TU in a PBS buffer solution was reported at pH level of 12.0, as shown in Fig. 4D.

3.4. Electrochemical detection of TU

Differential pulse voltammetry (DPV) analysis of 1.0×10^{-4} molL^{-1} of TU was investigated in 0.01molL^{-1} PBS for bare GCE, GCE/ZnONRs, and GCE/ZnONRs/Rutin as shown in Fig. 5A. In Fig. 5C compared the successive peak height was gradually increased with the modification of ZnO and Rutin on GCE surface. Therefore, ZnONRs/Rutin is proper mediator because of the shuttle electron between modified electrode and TU, like as exchanging electron. Similar research mechanism was reported by *Iraj Jodan and* et al., in their research work for the detection of TU in 0.1 molL^{-1} NaOH buffer solution [33]. In this study, the optimum pH 12.0 is selected for the oxidation of TU (Fig. 4E). At this pH oxidation of TU is done simultaneously disulfide bond formation of TU onto the chemisorbed rutin midified ZnONRs. The produced H^+ ion continuously accelerate this forwarding oxidation reaction with the production of $2H^+$ which is presented in Fig. S3. Manea et al. was reported the oxidation of TU at higher pH is suitable [6]. In this research work, the advantages is that at pH 12.0 the TU detection DPV peak will be vivid and increase the detection limit to lower value.

Additionally, successful DPV responses were monitored in the case of a different range of analytic concentration. It was observed that the oxidation current increases proportionally with increasing the concentration of TU in the range of 5.0×10^{-6} - 9.0×10^{-4} molL^{-1} by plotting the anodic peak. Therefore, an excellent correlation was maintained between TU concentrations and the oxidation current.

Furthermore, the linear concentration versus the obtained data using regression equation $y = 0.0321x + 0.046$, ($R^2 = 0.9995$). The limit of detection (LOD) was calculated by using the standard equation, LOD = 3 S/q [86]. Where, S is the standard deviation obtained from three measurement of blank measurement of modified GCE/ZnONRs/Rutin and q is the slope from the calibration of DPV measurements. The calculated LOD value is 2.0×10^{-6} molL^{-1}. This lower concentration revealed that the GCE/ZnONRs/Rutin electrochemical sensor denoted linearity and comparatively the lowest detection limit.

3.5. Selectivity, reproducibility, and stability study

To evaluate the practical application of the proposed electrochemical modified electrode, the interference study was significantly required. The selectivity of GCE/ZnONRs/Rutin sensor was investigated using a mixture of interfering salt solution (cation and anion) followed by DPV method. There was slight interference effect observed for the detection of TU by using (Na^+, Al^{2+}, Mg^{2+}, Ba^{2+}, K^+, $NO3^{2-}$, $SO4^{2-}$, Cl^-) medium for more than 200 fold. A negligible effect (less than 3 %) was observed using the developed sensor for the detection of TU in the presence of interfering salt solution. In the following step, a series of CV measurements were evaluated with the concentration of 5.0×10^{-5} and 1.0×10^{-5} molL^{-1} to determine the reproducibility and the calculated standard deviation at n = 3 were 0.3 and 0.2 %, respectively. That shows an outstanding reproducibility of the developed sensor. To evaluate the stability of the proposed sensor, the sensor was tested by storing at 4 °C for two weeks and then tested against 1×10^{-4} molL^{-1} of TU solution. No significant change (less than 1 %) was observed after two weeks indicating an excellent stability of the proposed sensor. The corresponding data is reported in supplementary information with Fig. S3. In Table 1, the polyphenol rutin functionalized Zinc oxide nanorod surface showed the excellent electrochemical response using DPV technique compared with other reported work for TU detection. Which is cheap, simple, short timing and comparatively better than other reported research work.

3.6. Detection of Thiourea in spiked real samples

The detection of TU in real sample is the most acceptable approach for evaluating the performance of the modified electrochemical sensor. The choice of TU media can easily influence the electrochemical detection. Hence, GCE/ZnONRs/Rutin modified electrode was utilized for the detection of TU in real samples such as farmland water and orange juice. To prepare a real sample, 20 ml of sample was centrifuged at 5000 rpm for 10 min. Thereafter, 1 ml of the supernatant was diluted to 10 ml by adding 0.01 molL^{-1} PBS at pH level of 12.0 by adding NaOH before the analysis.

Detection of TU in farmland water and orange juice is a standard addition method. 1.0×10^{-4} molL^{-1} of TU concentration are selected in both real sample experiments. Based on the data analysis, the recovery values were in the range of 98–99% as shown in Table 2. Furthermore, the relative standard deviation was satisfactory for the real sample medium supporting the main aspect of this research study.

4. Conclusions

In short, a newly developed GCE/ZnONRs/Rutin electrochemical sensor was used for selective detection of TU to overcome the complexity of conventional procedure. Differential pulse voltammetric techniques was used to obtain individual peak response of

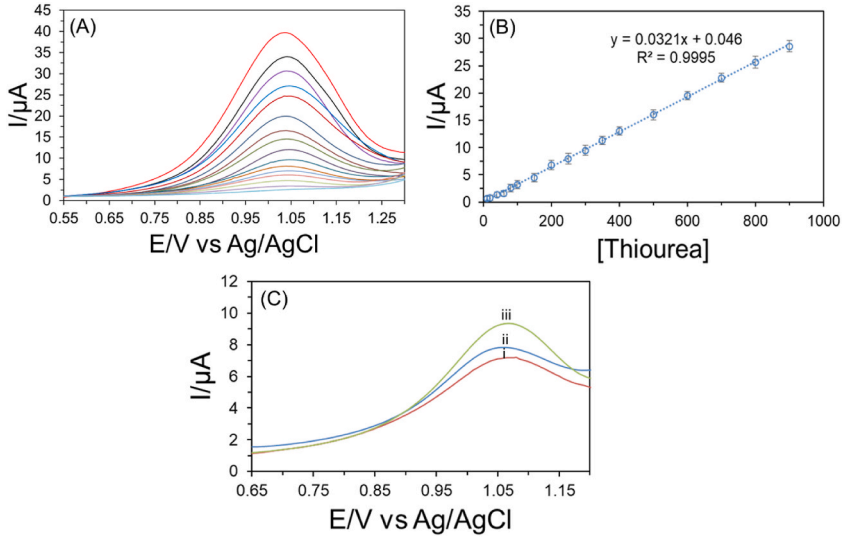

Fig. 5. DPV response by using the GCE/ZnONRs/Rutin in PBS solution (pH 12.0) for (A): concentration range from 5.0×10^{-6} - 9.0×10^{-4} molL^{-1}, (B): calibration curve of the measured different concentration of TU and (C): 100 μM of TU (i) bare GCE; (ii) GCE/ZnONRs; and (iii) GCE/ZnONRs/Rutin.

Table 1
Performance evaluation chart for the detection of TU using electrochemical sensor.

Electrode	Methods	**Linear range (molL^{-1})**	Detection limit (molL^{-1})	References
B-doped diamond electrode	CV	4.0×10^{-6}-4.0×10^{-3}	–	[87]
Ag NPs/AYP/GCE	DPV	1.0×10^{-5}-940×10^{-4}	3.3×10^{-6}	[33]
Ag NPs/AYP/GCE	CV	1.9×10^{-4}-1.1×10^{-3}	6.3×10^{-5}	[33]
GNSs-AgNPs/ILE	CV	1×10^{-6}-3.0×10^{-3}	7.0×10^{-7}	[26]
Alumina modified Pt	CV	2.5×10^{-5}-7.0×10^{-3}	4.8×10^{-6}	[1]
Pencil graphite electrode	SWV	6.3×10^{-6}-3.0×10^{-5}	1.29×10^{-6}	[87]
20 EG-PS (carbon based)	CV	1.0×10^{-4}-1.0×10^{-3}	2.0×10^{-5}	[88]
Nafion/CuO/ZnO NSs/GCE	DPV	1.5×10^{-4}-1.2×10^{-3}	$2.3 \pm 1.15 \times 10^{-5}$	[34]
AuE	CV	5.0×10^{-5}-1.0×10^{-3}	5.0×10^{-5}	[89]
Ag@CTSN/GCE	CV	2.00×10^{-4}–3.6×10^{-3}	1.8×10^{-5}	[35]
GCE/ZnO-Rutin	DPV	5.0×10^{-6}-9.0×10^{-4}	2.0×10^{-6}	This work

Table 2
Comparison of TU in four different real sample mediums.

Samples name	Added (molL^{-1})	Measured (mol L^{-1})	Recovery (%)	RSD (%)
Farmland water-I	1.0×10^{-4}	9.94×10^{-5}	99.4	0.29
Farmland water-I	5.0×10^{-5}	4.99×10^{-5}	99.7	0.27
Farmland water-I	2.0×10^{-6}	1.86×10^{-6}	99.06	0.37
Drain water-II	1.0×10^{-4}	9.95×10^{-5}	99.5	0.35
Drain water-II	5.0×10^{-5}	4.97×10^{-5}	99.8	0.30
Drain water-II	2.0×10^{-6}	1.91×10^{-6}	99.0	0.29
Mango juice	1.0×10^{-4}	9.87×10^{-5}	98.7	0.41
Mango juice	5.0×10^{-5}	4.89×10^{-5}	98.4	0.49
Mango juice	2.0×10^{-6}	1.83×10^{-6}	98.5	0.38
Orange juice	1.00×10^{-4}	9.91×10^{-5}	99.1	0.36
Orange juice	5.0×10^{-5}	4.91×10^{-5}	99.0	0.40
Orange juice	2.0×10^{-6}	1.96×10^{-6}	99.3	0.39

known TU concentration. Additionally, the modified GCE/ZnONRs/Rutin electrode exhibited higher electro catalytic activity for the proton exchange capacity of polyphenol rutin. The excellent linear range 5.0×10^{-6}-9.0×10^{-4} molL^{-1} and limit of detection 2.0×10^{-6} molL^{-1} evident that the polyphenol rutin modified electrode comparatively better than others reported work. Therefore, this study suggests that the developed sensor has a potential platform for the diagnosis of different biological samples as same as TU like properties. The electrode has a potential application for TU analysis in agricultural cultivating land with some limitations. Thus further extensive studies will be required for point-of-care applications with proper instrumentation of efficient electrochemical devices.

Funding statement

We appreciate the funding provided by Georgia Tech Shenzhen Institute (GTSI).

Data availability statement

Data will be made available on request.

CRediT authorship contribution statement

M.A. Khaleque: Formal analysis, Investigation, Validation, Visualization, Writing – original draft. **M.R. Ali:** Writing – review & editing. **M.S. Bacchu:** Validation, Visualization. **M.R.A. Mamun:** Writing – review & editing. **M.I. Hossain:** Visualization, Writing – review & editing. **M.S. Hossain:** Investigation, Visualization. **Mohamed Aly Saad Aly:** Conceptualization, Methodology, Project administration, Writing - original draft, Writing - review & editing. **M.Z.H. Khan:** Conceptualization, Project administration, Supervision, Writing – review & editing.

Declaration of competing interest

The authors declare that there is no conflict of interest.

Appendix A. Supplementary data

Supplementary data to this article can be found online at https://doi.org/10.1016/j.heliyon.2023.e20676.

References

[1] D. Nematollahi, M. Rafiee, Catalytic oxidation of thiourea at alumina modified Pt electrode, Sensors 3 (2003) 534–543, https://doi.org/10.3390/s31100534.
[2] A. Rosin, M. Rachmilewitz, The development of malignant tumors of the face in rats after prolonged treatment with thiourea, Cancer Res. 14 (1954) 494–496.
[3] L. Kanerva, T. Estlander, R. Jolanki, Occupational allergic contact dermatitis caused by thiourea compounds, Contact Dermatitis 31 (1994) 242–248, https://doi.org/10.1111/j.1600-0536.1994.tb01996.x.
[4] S.N. Giri, A.B. Combs, Sulfur-containing compounds and tolerance in the prevention of certain metabolic effects of phenylthiourea, Toxicol. Appl. Pharmacol. 16 (1970) 709–717, https://doi.org/10.1016/0041-008X(70)90076-1.
[5] R.J. Clark, G. Felsenfeld, © 1972 nature publishing group, Nat. New Biol. 240 (1972) 226–229, https://doi.org/10.1038/239137a0.
[6] F. Manea, C. Radovan, J. Schoonman, Amperometric determination of thiourea in alkaline media on a copper oxide-copper electrode, J. Appl. Electrochem. 36 (2006) 1075–1081, https://doi.org/10.1007/s10800-006-9152-9.
[7] S. Abbasi, H. Khani, M.B. Gholivand, A. Naghipour, A. Farmany, F. Abbasi, A kinetic method for the determination of thiourea by its catalytic effect in micellar media, Spectrochim. Acta Mol. Biomol. Spectrosc. 72 (2009) 327–331, https://doi.org/10.1016/j.saa.2008.09.029.
[8] C. Identity, E.W. Health, S. Controls, H.H. Information, R. Characterisation, Thiourea : Human Health Tier II Assessment CAS Number : 62-56-6 Thiocarbamide, 2020, pp. 1–13.
[9] K. Ziegler-Skylakakis, J. Kielhorn, G. Könnecker, J. Koppenhöfer, I. Mangelsdorf, Concise International Chemical Assessment Document 49: Thiourea, IPCS Concise International Chemical Assessment Documents, 2003.
[10] L. Tian, Y. Gao, L. Li, W. Wu, D. Sun, J. Lu, T. Li, Determination of thiourea using a carbon paste electrode decorated with copper oxide nanoparticles, Microchim. Acta 180 (2013) 607–612, https://doi.org/10.1007/s00604-013-0970-2.
[11] M.K. Upadhyay, A. Majumdar, A. Barla, S. Bose, S. Srivastava, f ur Pr pr oo, J. Hazard Mater. (2020), 124368, https://doi.org/10.1016/j.jhazmat.2020.124368.
[12] A. Wahid, S.M.A. Basra, M. Farooq, Thiourea, A molecule with immense biological significance for plants, Int. J. Agric. Biol. 19 (2017) 911–920, https://doi.org/10.17957/IJAB/15.0464.
[13] P. Yadav, S. Srivastava, Environmental Technology & Innovation Effect of thiourea application on root , old leaf and young leaf of two contrasting rice varieties (Oryza sativa L) grown in arsenic contaminated soil, Environ. Technol. Innov. 21 (2021), 101368, https://doi.org/10.1016/j.eti.2021.101368.
[14] N. Mansoora, S. Kausar, S.F. Amjad, S. Yaseen, H. Shahid, K. tul Kubra, S.A.M. Alamri, S.A. Alrumman, E.M. Eid, G. Mustafa, S.A. Ali, S. Danish, Application of sewage sludge combined with thiourea improves the growth and yield attributes of wheat (Triticum aestivum L.) genotypes under arsenic-contaminated soil, PLoS One 16 (2021) 1–15, https://doi.org/10.1371/journal.pone.0259289.
[15] I. Ashraf, T. Khan, N. Rashid, S. Ramzan, Role of Some Emerging Agro-Chemicals in Groundwater Contamination Chapter 2 Role of Some Emerging Agro-Chemicals in Groundwater Contamination, 2019, https://doi.org/10.26832/AESA-2019-CAE-0168-02.
[16] Y.L. Cao, Y. Li, F. Zhang, J.Z. Huo, X.J. Zhao, Highly sensitive “naked-eye” colorimetric detection of thiourea using gold nanoparticles, Anal. Methods 7 (2015) 4927–4933, https://doi.org/10.1039/c5ay00558b.
[17] J. Kurzawa, K. Janowicz, Use of a stopped-flow technique for investigation and determination of thiourea and its N-methyl derivatives as inducers of the iodine-azide reaction, Anal. Bioanal. Chem. 382 (2005) 1584–1589, https://doi.org/10.1007/s00216-005-3372-4.
[18] H.J. Bowley, E.A. Crathorne, D.L. Gerrard, Quantitative determination of thiourea in aqueous solution in the presence of sulphur dioxide by Raman spectroscopy, Analyst 111 (1986) 539–542, https://doi.org/10.1039/AN9861100539.
[19] S. Abbasi, H. Khani, L. Hosseinzadeh, Z. Safari, Determination of thiourea in fruit juice by a kinetic spectrophotometric method, J. Hazard Mater. 174 (2010) 257–262, https://doi.org/10.1016/j.jhazmat.2009.09.045.
[20] A. Raffaelli, S. Pucci, R. Lazzaroni, P. Salvadori, Rapid determination of thiourea in waste water by atmospheric pressure chemical ionization tandem mass spectrometry using selected-reaction monitoring, Rapid Commun. Mass Spectrom. 11 (1997) 259–264, https://doi.org/10.1002/(sici)1097-0231 (19970215) 11:3<259::aid-rcm826>3.0.co;2-%23.
[21] M.R. Smyth, J.G. Osteryoung, Determination of some thiourea-containing pesticides by pulse voltammetric methods of analysis, Anal. Chem. 49 (1977) 2310–2314, https://doi.org/10.1021/ac50022a050.
[22] V. Stará, M. Kopanica, Adsorptive stripping voltammetric determination of thiourea and thiourea derivatives, Anal. Chim. Acta 159 (1984) 105–110, https://doi.org/10.1016/S0003-2670(00)84286-5.

[23] J. Rethmeier, G. Neumann, C. Stumpf, A. Rabenstein, C. Vogt, Determination of low thiourea concentrations in industrial process water and natural samples using reversed-phase high-performance liquid chromatography, J. Chromatogr. A 934 (2001) 129–134, https://doi.org/10.1016/S0021-9673(01)01289-4.

[24] K. Kargosha, M. Khanmohammadi, M. Ghadiri, Fourier transform infrared spectrometric determination of thiourea in the presence of sulphur dioxide in aqueous solution, Anal. Chim. Acta 437 (2001) 139–143, https://doi.org/10.1016/S0003-2670(01)00943-6.

[25] A. Tashdjian, M.G. SánchezLoredo, G.A. González, Preparation of silver nanoparticles-based sensors for the electrochemical detection of thiourea in leaching solutions of waste electrical and electronic equipment, Electroanalysis 25 (2013) 2124–2129, https://doi.org/10.1002/elan.201300242.

[26] A. Safavi, R. Ahmadi, F.A. Mahyari, M. Tohidi, Electrocatalytic oxidation of thiourea on graphene nanosheets-Ag nanoparticles hybrid ionic liquid electrode, Sens. Actuators, B (2015) 668–672, https://doi.org/10.1016/j.snb.2014.10.057.

[27] G. Li, X. Qi, G. Zhang, S. Wang, K. Li, J. Wu, Low-cost Voltammetric Sensors for Robust Determination of Toxic Cd (II) and Pb (II) in Environment and Food Based on Shuttle-like α -Fe 2 O 3 Nanoparticles Decorated β -Bi 2 O 3 Microspheres, 2022, p. 179.

[28] Q. Li, J. Wu, Y. Liu, X. Qi, H. Jin, C. Yang, Analytica Chimica Acta Recent advances in black phosphorus-based electrochemical sensors : a review, Anal. Chim. Acta 1170 (2021), 338480, https://doi.org/10.1016/j.aca.2021.338480.

[29] G. Li, J. Wu, X. Qi, X. Wan, Y. Liu, Y. Chen, L. Xu, Ethylenedioxythiophene): polystyrene sulfonate-functionalized black phosphorene for the selective and robust detection of nor fl oxacin, Mater. Today Chem. 26 (2022), 101043, https://doi.org/10.1016/j.mtchem.2022.101043.

[30] M. Rohani Moghadam, S. Akbarzadeh, N. Nasirizadeh, Electrochemical sensor for the determination of thiourea using a glassy carbon electrode modified with a self-assembled monolayer of an oxadiazole derivative and with silver nanoparticles, Microchim. Acta 183 (2016) 1069–1077, https://doi.org/10.1007/s00604-015-1723-1.

[31] M.A. Khaleque, M.S. Bacchu, M.R. Ali, M.S. Hossain, M.R.A. Mamun, Heliyon Copper oxide nanoflowers/poly- L -glutamic acid modified advanced electrochemical sensor for selective detection of L -tryptophan in real samples, Heliyon 9 (2023), e16627, https://doi.org/10.1016/j.heliyon.2023.e16627.

[32] S. Hossain, A. Khaleque, R. Ali, S. Bacchu, I. Hossain, M. Aly, S. Aly, Z.H. Khan, Poly (3 , 4-ethylenedioxythiophene): Polystyrene Sulfonate-Modified Electrode for the Detection of Furosemide in Pharmaceutical Products, 2023, https://doi.org/10.1021/acsomega.3c00463.

[33] I. Jodan, K. Wantala, N. Amini, B. Shahmoradi, M. Ghaslani, S.M. Lee, J. Yang, S.H. Puttaiah, Fabrication of a sensitive electrochemical sensor based on Ag nanoparticles and alizarin yellow polymer: application to the detection of an environmental pollutant thiourea, Kor. J. Chem. Eng. 37 (2020) 1609–1615, https://doi.org/10.1007/s11814-020-0561-y.

[34] M.M. Rahman, M.M. Alam, S.Y.M. Alfaifi, A.M. Asiri, M.M. Ali, Sensitive detection of thiourea hazardous toxin with sandwich-type nafion/cuo/zno nanospikes/glassy carbon composite electrodes, Polymers 13 (2021), https://doi.org/10.3390/polym13223998.

[35] M.A. Rashed, J. Ahmed, M. Faisal, S.A. Alsareii, M. Jalalah, F.A. Harraz, Highly sensitive and selective thiourea electrochemical sensor based on novel silver nanoparticles/chitosan nanocomposite, Colloids Surf. A Physicochem. Eng. Asp. 644 (2022), 128879, https://doi.org/10.1016/j.colsurfa.2022.128879.

[36] M.A. Khaleque, M.I. Hossain, M.Z.H. Khan, Nanostructured Wearable Electrochemical and Biosensor towards Healthcare Management : a Review, 2023, pp. 22973–22997, https://doi.org/10.1039/d3ra03440b.

[37] R. Ali, S. Bacchu, R. Al-mamun, I. Hossain, A. Khaleque, Recent advanced in MXene research toward iosensor development, Crit. Rev. Anal. Chem. 0 (2022) 1–18, https://doi.org/10.1080/10408347.2022.2115286.

[38] R.M. Hanabaratti, S.M. Tuwar, S.T. Nandibewoor, J.I. Gowda, Fabrication and characterization of zinc oxide nanoparticles modified glassy carbon electrode for sensitive determination of paracetamol, Chemical Data Collections 30 (2020), https://doi.org/10.1016/j.cdc.2020.100540.

[39] M. Daizy, M.R. Ali, M.S. Bacchu, M.A.S. Aly, M.Z.H. Khan, ZnO hollow spheres arrayed molecularly-printed-polymer based selective electrochemical sensor for methyl-parathion pesticide detection, Environ. Technol. Innov. 24 (2021), 101847, https://doi.org/10.1016/j.eti.2021.101847.

[40] Shahid-ul-Islam, B.S. Butola, A. Kumar, Green chemistry based in-situ synthesis of silver nanoparticles for multifunctional finishing of chitosan polysaccharide modified cellulosic textile substrate, Int. J. Biol. Macromol. 152 (2020) 1135–1145, https://doi.org/10.1016/j.ijbiomac.2019.10.202.

[41] S. Bargozideh, M. Tasviri, M. Ghabraei, Effect of carbon nanotubes loading on the photocatalytic activity of BiSI/BiOI as a novel photocatalyst, Environ. Sci. Pollut. Control Ser. 27 (2020) 36754–36764, https://doi.org/10.1007/s11356-020-09759-0.

[42] Q. Wang, J. Zheng, Electrodeposition of silver nanoparticles on a zinc oxide film: improvement of amperometric sensing sensitivity and stability for hydrogen peroxide determination, Microchim. Acta 169 (2010) 361–365, https://doi.org/10.1007/s00604-010-0356-7.

[43] L. Yang, W. Zhang, M. Duan, Z. Jin, Electrodeposition of porous ZnO electrodes in the presence of cetyltrimethylammonium bromide, Adv. Mater. Res. 105–106 (2010) 639–642. https://doi.org/10.4028/www.scientific.net/AMR.105-106.639.

[44] D. da Silva Biron, V. dos Santos, C.P. Bergmann, Synthesis and characterization of zinc oxide obtained by combining zinc nitrate with sodium hydroxide in polyol medium, Mater. Res. 23 (2020) 1–6, https://doi.org/10.1590/1980-5373-MR-2020-0080.

[45] M. Amare, W. Teklay, Voltammetric determination of paracetamol in pharmaceutical tablet samples using anthraquinone modified carbon paste electrode, Cogent Chemistry 5 (2019), 1576349, https://doi.org/10.1080/23312009.2019.1576349.

[46] C. Tang, S.A. Kumar, S. Chen, sp ww w . m . 380 (2008) 174–183, https://doi.org/10.1016/j.ab.2008.06.004.

[47] S.R.K. Kumar, K.Y. Kumar, H.B. Muralidhara, M.S. Anantha, G.P. Mamatha, ScienceDirect Synthesis and characterization of Hierarchically assembled ZnO Nanoparticles and its application in modified carbon paste electrode for electrochemical detection of Biomolecules, Mater. Today: Proc. 5 (2018) 20947–20954, https://doi.org/10.1016/j.matpr.2018.06.484.

[48] M. Luqman, M. Napi, A. Fakhrurrazi, A. Noorden, M. Loong, P. Tan, H. Jamaluddin, F.A. Hamid, M.K. Ahmad, U. Hashim, M.R. Ahmad, S.M. Sultan, Review — Three Dimensional Zinc Oxide Nanostructures as an Active Site Platform for Biosensor : Recent Trend in Healthcare Diagnosis Review — Three Dimensional Zinc Oxide Nanostructures as an Active Site Platform for Biosensor : Recent Trend in Healthcare, (n.d.) https://doi.org/10.1149/1945-7111/abb4f4..

[49] M. Zidan, Electrochemical Oxidation of Paracetamol Mediated by Zinc Oxide Modified Glassy Carbon Electrode Electrochemical Oxidation of Paracetamol Mediated by Zinc Oxide Modified Glassy Carbon Electrode, 2010.

[50] S.D. Bukkitgar, N.P. Shetti, R.M. Kulkarni, M.R. Doddamani, Electro-oxidation of nimesulide at 5 % barium-doped zinc oxide nanoparticle modi fi ed glassy carbon electrode, JEAC 762 (2016) 37–42, https://doi.org/10.1016/j.jelechem.2015.12.023.

[51] M. Moyo, L.R. Florence, J.O. Okonkwo, Sensors and Actuators B : chemical Improved electro-oxidation of triclosan at nano-zinc oxide-multiwalled carbon nanotube modified glassy carbon electrode, Sensor. Actuator. B Chem. 209 (2015) 898–905, https://doi.org/10.1016/j.snb.2014.12.059.

[52] N. Ait, A. Houa, H. Marielle, E. Carine, C. Florence, P. Knauth, L. Makhloufi, Voltammetric determination of ascorbic acid with zinc oxide modified glassy carbon electrode, J. Iran. Chem. Soc. (2019), https://doi.org/10.1007/s13738-019-01668-5.

[53] N. Ahmed, H. Houa, M. Eyraud, C. Chassigneux, F. Vacandio, P. Knauth, L. Makhloufi, N. Gabouze, N. Ahmed, H. Houa, M. Eyraud, C. Chassigneux, F. Vacandio, Voltammetric Determination of Ascorbic Acid with Zinc Oxide Modified Glassy Carbon Electrode to Cite This Version : HAL Id : Hal-02470781, 2020.

[54] X. Zhang, Y. Zhang, L. Ma, Sensors and Actuators B : chemical One-pot facile fabrication of graphene-zinc oxide composite and its enhanced sensitivity for simultaneous electrochemical detection of ascorbic acid , dopamine and uric acid, Sensor. Actuator. B Chem. 227 (2016) 488–496, https://doi.org/10.1016/j.snb.2015.12.073.

[55] Y. Xia, G. Li, Y. Zhu, Q. He, C. Hu, Facile preparation of metal-free graphitic-like carbon nitride/graphene oxide composite for simultaneous determination of uric acid and dopamine, Microchem. J. 190 (2023), 108726, https://doi.org/10.1016/j.microc.2023.108726.

[56] S. Palanisamy, A.T.E. Vilian, S. Chen, Direct electrochemistry of glucose oxidase at reduced graphene oxide/zinc oxide composite modified electrode for glucose, Sensors 7 (2012) 2153–2163.

[57] F. Li, B. Ni, Y. Zheng, Y. Huang, G. Li, A simple and efficient voltammetric sensor for dopamine determination based on ZnO nanorods/electro-reduced graphene oxide composite, Surface. Interfac. 26 (2021), 101375, https://doi.org/10.1016/j.surfin.2021.101375.

[58] M.A. Ansari, M. Murali, D. Prasad, M.A. Alzohairy, A. Almatroudi, M.N. Alomary, A.C. Udayashankar, S.B. Singh, S.M.M. Asiri, B.S. Ashwini, H.G. Gowtham, N. Kalegowda, K.N. Amruthesh, T.R. Lakshmeesha, S.R. Niranjana, Cinnamomum verum bark extract mediated green synthesis of ZnO nanoparticles and their antibacterial potentiality, Biomolecules 10 (2020), https://doi.org/10.3390/biom10020336.

[59] P.A. Luque, C.A. Soto-Robles, O. Nava, C.M. Gomez-Gutierrez, A. Castro-Beltran, H.E. Garrafa-Galvez, A.R. Vilchis-Nestor, A. Olivas, Green synthesis of zinc oxide nanoparticles using Citrus sinensis extract, J. Mater. Sci. Mater. Electron. 29 (2018) 9764–9770, https://doi.org/10.1007/s10854-018-9015-2.

[60] D. Bharathi, V. Bhuvaneshwari, Synthesis of zinc oxide nanoparticles (ZnO NPs) using pure bioflavonoid rutin and their biomedical applications: antibacterial, antioxidant and cytotoxic activities, Res. Chem. Intermed. 45 (2019) 2065–2078, https://doi.org/10.1007/s11164-018-03717-9.
[61] M. Keyvanfard, Z. Jalilian, H. Karimi-Maleh, K. Alizad, Voltammetric determination of glutathionein pharmaceutical and biological samples using multiwall carbon nanotubes paste electrode in the presence of rutin as a mediator, Iran. J. Pharm. Res. (IJPR) 19 (2020) 251–258, https://doi.org/10.22037/ijpr.2016.1947.
[62] Ş. Ulubay, C. Koçak, Z. Dursun, An Over-oxidized Poly (Rutin) Modi Fi Ed Electrode for Selective and Sensitive Determination of Catechol and Hydroquinone, 2019, p. 850, https://doi.org/10.1016/j.jelechem.2019.113415.
[63] C. Madhuri, Y.V. Manoharreddy, D. Saritha, M. Venu, S. Kiranmai, V.P. Rao, G. Madhavi, Electrochemical behavior of poly (rutin) modified carbon paste electrode for the determination of uric acid in the presence of ascorbic, Acid and Dopamine 5 (2016) 136–143.
[64] G. Jin, Q. Chen, Y. Ding, J. He, Electrochemistry behavior of adrenalin , serotonin and ascorbic acid at novel poly rutin modified paraffin-impregnated graphite electrode 52 (2007) 2535–2541, https://doi.org/10.1016/j.electacta.2006.08.068.
[65] S. Mustapha, M.M. Ndamitso, A.S. Abdulkareem, J.O. Tijani, D.T. Shuaib, A.K. Mohammed, A. Sumaila, Comparative study of crystallite size using Williamson-Hall and Debye-Scherrer plots for ZnO nanoparticles, Adv. Nat. Sci. Nanosci. Nanotechnol. 10 (2019), https://doi.org/10.1088/2043-6254/ab52f7.
[66] G. Iannaccone, A. Bernardi, R. Suriano, C.L. Bianchi, M. Levi, S. Turri, G. Griffini, The role of sol-gel chemistry in the low-temperature formation of ZnO buffer layers for polymer solar cells with improved performance, RSC Adv. 6 (2016) 46915–46924, https://doi.org/10.1039/c6ra03344j.
[67] T.U. Doan Thi, T.T. Nguyen, Y.D. Thi, K.H. Ta Thi, B.T. Phan, K.N. Pham, Green synthesis of ZnO nanoparticles using orange fruit peel extract for antibacterial activities, RSC Adv. 10 (2020) 23899–23907, https://doi.org/10.1039/d0ra04926c.
[68] K.R. Ahammed, M. Ashaduzzaman, S.C. Paul, M.R. Nath, S. Bhowmik, O. Saha, M.M. Rahaman, S. Bhowmik, T. Das Aka, Microwave assisted synthesis of zinc oxide (ZnO) nanoparticles in a noble approach: utilization for antibacterial and photocatalytic activity, SN Appl. Sci. 2 (2020), https://doi.org/10.1007/s42452-020-2762-8.
[69] J. Suresh, G. Pradheesh, V. Alexramani, M. Sundrarajan, S.I. Hong, Green synthesis and characterization of zinc oxide nanoparticle using insulin plant (Costus pictus D. Don) and investigation of its antimicrobial as well as anticancer activities, Adv. Nat. Sci. Nanosci. Nanotechnol. 9 (2018), https://doi.org/10.1088/2043-6254/aaa6f1.
[70] S.M. Taghizadeh, N. Lal, A. Ebrahiminezhad, F. Moeini, M. Seifan, Y. Ghasemi, A. Berenjian, Green and economic fabrication of zinc oxide (ZnO) nanorods as a broadband UV blocker and antimicrobial agent, Nanomaterials 10 (2020) 1–12, https://doi.org/10.3390/nano10030530.
[71] S. Mahalakshmi, N. Hema, P.P. Vijaya, In vitro biocompatibility and antimicrobial activities of zinc oxide nanoparticles (ZnO NPs) prepared by chemical and green synthetic route— a comparative study, BioNanoScience 10 (2020) 112–121, https://doi.org/10.1007/s12668-019-00698-w.
[72] A. Koodziejczak-Radzimska, E. Markiewicz, T. Jesionowski, Structural characterisation of ZnO particles obtained by the emulsion precipitation method, J. Nanomater. (2012) 2012, https://doi.org/10.1155/2012/656353.
[73] S.N. Cuo, Z. Nanospikes, G. Carbon, Sensitive Detection of Thiourea Hazardous Toxin with, 2021.
[74] H. Mohd Yusof, N.A. Abdul Rahman, R. Mohamad, U.H. Zaidan, A.A. Samsudin, Biosynthesis of zinc oxide nanoparticles by cell-biomass and supernatant of Lactobacillus plantarum TA4 and its antibacterial and biocompatibility properties, Sci. Rep. 10 (2020) 1–13, https://doi.org/10.1038/s41598-020-76402-w.
[75] A. Ebrahiminezhad, F. Moeeni, S.M. Taghizadeh, M. Seifan, C. Bautista, D. Novin, Y. Ghasemi, A. Berenjian, Xanthan gum capped ZnO microstars as a promising dietary zinc supplementation, Foods 8 (2019) 1–10, https://doi.org/10.3390/foods8030088.
[76] I. Ahmad, Comparative study of metal (Al, Mg, Ni, Cu and Ag) doped ZnO/g-C3N4 composites: efficient photocatalysts for the degradation of organic pollutants, Sep. Purif. Technol. 251 (2020), 117372, https://doi.org/10.1016/j.seppur.2020.117372.
[77] S. Suzer, H. Sezen, A. Dâna, Two-dimensional X-ray photoelectron spectroscopy for composite surface analysis, Anal. Chem. 80 (2008) 3931–3936, https://doi.org/10.1021/ac702642w.
[78] O. Galmiz, M. Stupavska, H. Wulff, H. Kersten, A. Brablec, M. Cernak, Deposition of Zn-containing films using atmospheric pressure plasma jet, Open Chem. 13 (2015) 198–203, https://doi.org/10.1515/chem-2015-0020.
[79] R. Al-Gaashani, S. Radiman, A.R. Daud, N. Tabet, Y. Al-Douri, XPS and optical studies of different morphologies of ZnO nanostructures prepared by microwave methods, Ceram. Int. 39 (2013) 2283–2292, https://doi.org/10.1016/j.ceramint.2012.08.075.
[80] M. Claros, M. Setka, Y.P. Jimenez, S. Vallejos, Aacvd synthesis and characterization of iron and copper oxides modified zno structured films, Nanomaterials 10 (2020) 1–16, https://doi.org/10.3390/nano10030471.
[81] K. Geunjae, Y. Kijung, Adsorption and reaction of ethanol on ZnO nanowires, J. Phys. Chem. C 112 (2008) 3036–3041, https://doi.org/10.1021/jp7103819.
[82] H. Adkins, W.A. Lazier, The reactions of the alcohols over zinc oxide catalysts, J. Am. Chem. Soc. 48 (1926) 1671–1677, https://doi.org/10.1021/ja01417a031.
[83] A. Šarić, I. Despotović, G. Štefanić, Alcoholic solvent influence on ZnO synthesis: a joint experimental and theoretical study, J. Phys. Chem. C 123 (2019) 29394–29407, https://doi.org/10.1021/acs.jpcc.9b07411.
[84] R. Ahmad, K.S. Bhat, M.S. Ahn, Y.B. Hahn, Fabrication of a robust and highly sensitive nitrate biosensor based on directly grown zinc oxide nanorods on a silver electrode, New J. Chem. 41 (2017), 10992, https://doi.org/10.1039/c7nj02526b. –10997.
[85] Q. Yuan, Z. Zhang, L. Li, Electrochemical sensor based on glassy carbon electrode modified by palladium doped ZnO nanostructures for glucose detection, Int. J. Electrochem. Sci. 15 (2020) 5245–5254, https://doi.org/10.20964/2020.06.80.
[86] L. Zhang, M. Yin, J. Qiu, T. Qiu, Y. Chen, S. Qi, X. Wei, X. Tian, D. Xu, An electrochemical sensor based on CNF@AuNPs for metronidazole hypersensitivity detection, Biosens. Bioelectron. X. 10 (2022), 100102, https://doi.org/10.1016/j.biosx.2021.100102.
[87] N. Spataru, T. Spataru, A. Fujishima, Voltammetric determination of thiourea at conductive diamond electrodes, Electroanalysis 17 (2005) 800–805, https://doi.org/10.1002/elan.200403139.
[88] I. Corb, F. Manea, C. Radovan, A. Pop, G. Burtica, P. Malchev, S. Picken, J. Schoonman, Carbon-based composite electrodes: preparation, characterization and application in electroanalysis, Sensors 7 (2007) 2626–2635, https://doi.org/10.3390/s7112626.
[89] J. Lee, S. Mho, C.H. Pyun, Flow Injective Determination of Thiourea by Amperometry 15 (1994) 1038–1042.